Modelling Simul. Mater. Sci. Eng. **8** (2000) 497–513. Printed in the UK PII: S0965-0393(00)14481-X

Modelling and experimental analysis of vacuum plasma spraying. Part I: prediction of initial plasma properties at plasma gun exit

Y Y Zhao†, P S Grant and B Cantor

Oxford Centre for Advanced Materials and Composites, Department of Materials, University of Oxford, Parks Road, Oxford OX1 3PH, UK

E-mail: y.y.zhao@liv.ac.uk

Received 2 January 2000, accepted for publication 31 May 2000

Abstract. The plasma energy input rate of a dc Ar + H_2 plasma jet has been measured experimentally under a series of vacuum plasma spraying (VPS) processing conditions. The plasma energy input rate increased approximately linearly with increasing plasma current and Ar flow rate, increased approximately parabolically with increasing H_2 flow rate, but did not vary measurably with changes in VPS chamber pressure. Based on these experimental results, an approximate analytical model has been developed to calculate the initial plasma gas temperature, degrees of Ar and H ionization and the plasma gas velocity at the plasma gun exit as functions of the VPS processing parameters of plasma current, Ar flow rate, H_2 flow rate and chamber pressure. The model is based on an energy balance in the plasma gas between the input electrical energy and the energy consumed by gas dissociation, ionization and heating. In part II of this paper, the model is used to predict the boundary conditions for a subsequent computational fluid dynamics model of plasma gas and particle flow during VPS.

Nomenclature

C_{Ar}	specific heat of Ar
C_{H_2}	specific heat of H_2
C_w	specific heat of water
$\dot{E}$	energy input rate
$\dot{E}_h$	heating energy consumption rate
$\dot{E}_i$	dissociation and ionization energy consumption rate
$\dot{E}_l$	energy loss rate
F_{Ar}	Ar flow rate
F_{H_2}	H_2 flow rate
F_w	molar flow rate of plasma gun cooling water
I	plasma current
K_1	constant
K_2	constant
K_3	constant

† Present address: Materials Science and Engineering, Department of Engineering, The University of Liverpool, Brownlow Hill, Liverpool L69 3GH, UK.

0965-0393/00/040497+17$30.00 © 2000 IOP Publishing Ltd

k	constant
k_i	constant
k_d	constant
P	plasma gas pressure
P_0	plasma gas pressure at plasma gun exit
Q	dissociation or ionization energy
Q_{Ar}	ionization energy of Ar
Q_H	ionization energy of H
Q_{H_2}	dissociation energy of H_2
R	gas constant
S	cross sectional area of plasma gun exit orifice
T	plasma gas temperature
T_0	initial plasma temperature at plasma gun exit
T_r	room temperature
T_w	temperature of cooling water leaving plasma gun
T_{w_0}	temperature of cooling water entering plasma gun
v	plasma gas velocity
χ	degree of dissociation or ionization
χ_{Ar}	degree of ionization of Ar
χ_H	degree of ionization of H
χ_{H_2}	degree of dissociation of H_2

1. Introduction

Atmospheric and vacuum plasma spraying (APS and VPS) are widely used to produce coatings of high melting point and highly reactive materials, and may also be used to manufacture particulate or fibre-reinforced ceramic or metal matrix composite deposits [1–8]. The benefits of plasma spraying include [1–13]:

(1) high plasma jet temperatures make it possible to spray any particulate material including metals, refractories and ceramics;
(2) high droplet cooling rates (10^4–10^6 K s^{-1}) at deposition promote rapid solidification benefits such as small matrix grain size, uniform composition and extended solid solubility;
(3) high particle velocities at deposition promote dense deposits; and
(4) the inert, low pressure atmosphere in VPS allows reactive metals such as Ti to be sprayed without excessive oxidation.

The microstructure and mechanical properties of VPS protective coatings and composite deposits are determined by the sizes, temperatures and velocities of the droplets in the spray at deposition, which in turn are determined by the plasma jet characteristics, i.e. the spatial distribution of plasma gas temperature and velocity, and the degrees of dissociation and ionization. The temperature and velocity fields depend largely on the initial plasma gas properties at the plasma gun exit orifice. If the initial plasma gas temperature, velocity and degrees of dissociation and ionization are known, the subsequent spatial distribution of plasma gas temperature and velocity in the plasma jet may be modelled [14–22]. These types of models provide insight into the underlying physics governing the plasma spraying process where experimental measurements are difficult.

In VPS, the relationship between the processing conditions and the resulting plasma and particle properties is complex because of the large number of processing parameters,

including plasma current, plasma gas composition and flow rate, chamber pressure, powder size, powder feed rate, carrier gas flow rate, spray distance and plasma gun traversing speed. The optimization of the spraying processes has been developed largely by empirical means, and complete scientific understanding of the physical mechanisms controlling plasma gas temperatures and velocities and their effect on subsequent particle behaviour in the spray is lacking [23–25].

This paper is part I of a two part series. Part I describes: (1) an experimental investigation into the effect of VPS processing parameters such as plasma current, primary Ar flow rate, secondary H_2 flow rate and chamber pressure on the plasma energy input rate of an Ar + H_2 plasma; and (2) an analytical model to calculate the initial plasma gas temperature, velocity and degrees of Ar and H ionization at the plasma gun exit as functions of these VPS processing parameters. In part II, a computational fluid dynamics model is described to calculate the spatial distributions of plasma gas temperature, fractions of dissociated and ionized gases and plasma gas velocity as well as particle trajectory, temperature and velocity in the plasma jet using commercial software, FLUENT V4.2†, with modifications to incorporate the effect of the plasma. The effect of processing conditions is investigated using predictions of the initial plasma properties at the plasma gun exit described in this paper as boundary conditions.

2. Experiment

All VPS experiments were performed using a Plasma Technik (now Sulzer Metco) A2000 system as shown schematically in figure 1. The spray chamber was evacuated to below 10 Pa, and then back filled with Ar to 5 to 25 kPa. A potential difference of 30–80 V was applied across the tungsten cathode and the copper anode of a PT-F4 plasma gun. With the plasma gas flowing between the two electrodes, a direct current (dc) arc was initiated and stabilized, which created and maintained a hot plasma jet exiting from the plasma gun. The plasma gas consisted of a mixture of primary Ar and secondary H_2, the composition of which was varied by adjusting the Ar and H_2 flow rates independently. No powder was fed into the plasma gun, but a pure Ar carrier gas flowed through the two powder feed tubes to approximate powder spraying conditions, and to cool the feed tubes. Typical operating conditions were: plasma current 700 A, primary Ar flow rate 35 l min^{-1}, secondary H_2 flow rate 8 l min^{-1}, chamber pressure 15 kPa and carrier gas flow rate 1.6 l min^{-1}. In this paper, volume flow rates of gases are expressed under standard conditions, i.e. at a pressure of 1.053×10^5 Pa and a temperature of 298 K, and can be converted into molar flow rates (mol s^{-1}) by multiplying by 7.08×10^{-4}. The different spraying parameters were varied independently to investigate their effects on the plasma energy input rate. Plasma arc voltage and current were measured directly and displayed on the PT-A2000 console, from which the plasma energy input rate was calculated. The thermal loss through the plasma gun carried away by the cooling water was approximated by measuring the temperature and the flow rate of the cooling water flowing in and out of the plasma gun during operation.

3. Model

3.1. Plasma energy balance

The precise prediction of the temperature and velocity profile of a plasma gas mixture leaving a plasma gun orifice is difficult because of the complex internal geometry of a plasma gun and

† FLUENT is a registered trademark of FLUENT Inc., Centerra Resource Park, 10 Cavendish Court, Lebanon, NH 03766, USA.

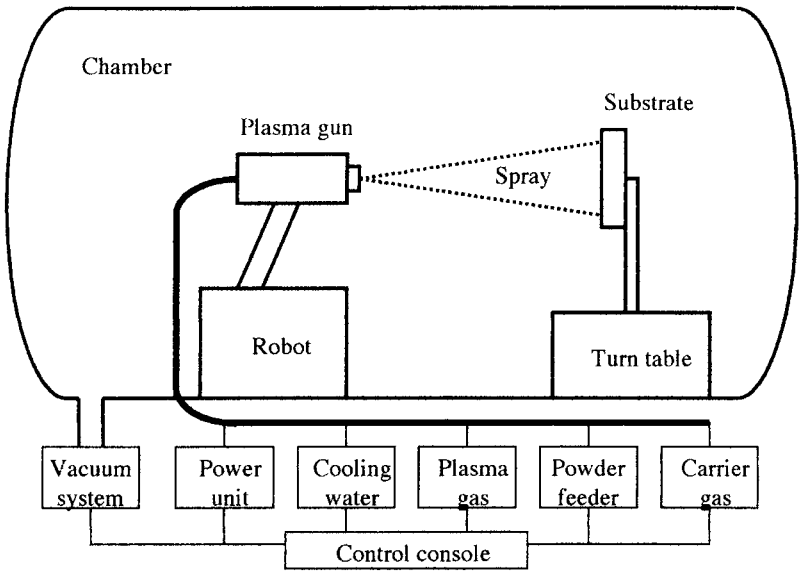

Figure 1. Schematic of the Plasma Technik A2000 VPS system.

uncertainties in the physical properties of a hot plasma. In this model subsequently described to calculate the initial plasma temperature, velocity and degrees of dissociation and ionization, the following assumptions were made:

(1) the plasma is in local thermodynamic equilibrium, i.e. the temperatures of the gas atoms, ions and electrons at a point are equal [26, 27], and therefore can be characterized by a single temperature;

(2) the degrees of dissociation and ionization as functions of temperature and pressure follow the Saha equation [28, 29];

(3) the specific heat of Ar^+ is equal to that of Ar and the specific heats of both H and H^+ are equal to half of the specific heat of H_2 at all temperatures [26];

(4) the energy loss by radiation is negligible [9];

(5) the ideal gas law is applicable; and

(6) the plasma gas temperature and velocity do not vary across the plasma gun orifice.

All these assumptions are simplifications of the likely real case, but allow conversion of measured plasma arc conditions into initial plasma properties. It is further assumed that the input energy into the plasma gases in the plasma gun at steady state is consumed by: (1) losses through the plasma gun to the cooling water, (2) dissociation and ionization of the gases, and (3) heating of the gases. For plasma gases flowing through the plasma gun nozzle, the energy balance is

$$\dot{E} = \dot{E}_{\mathrm{l}} + \dot{E}_{\mathrm{i}} + \dot{E}_{\mathrm{h}} \tag{1}$$

where $\dot{E}$ is the energy input rate, $\dot{E}_{\mathrm{l}}$ is the energy loss rate to the plasma gun cooling water, $\dot{E}_{\mathrm{i}}$ is the dissociation and ionization energy consumption rate, and $\dot{E}_{\mathrm{h}}$ is the heating energy consumption rate.

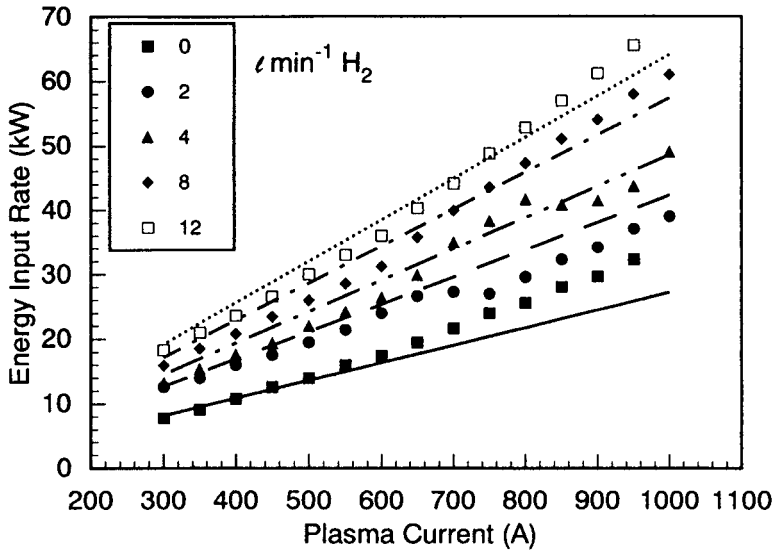

Figure 2. Relationship between plasma energy input rate and plasma current.

3.2. Energy input rate $\dot{E}$

The electrical energy input rate $\dot{E}$ is the product of plasma current and plasma arc voltage. Experimental measurements of plasma arc voltage under a series of VPS processing conditions were performed by systematically varying the plasma current, Ar flow rate, H_2 flow rate and chamber pressure over the ranges: 300–1000 A, 15–50 l min^{-1}, 0–14 l min^{-1} and 5–35 kPa, respectively. Figure 2 shows the variations of energy input rate with plasma current in the range 300–1000 A for different H_2 flow rates, with a fixed Ar flow rate of 35 l min^{-1} and chamber pressure of 15 kPa. The energy input rate is approximately proportional to plasma current, because plasma arc voltage does not vary very much with varying plasma current. Figure 3 shows the variations of energy input rate with Ar flow rate in the range 15–50 l min^{-1} for different plasma currents of 300, 500, 700 and 900 A, respectively, with a fixed H_2 flow rate of 8 l min^{-1} and chamber pressure of 15 kPa. With a given plasma current, the energy input rate increases almost linearly with increasing Ar flow rate. Figure 4 shows the variations of energy input rate with H_2 flow rate in the range 0–14 l min^{-1} for different plasma currents of 300, 500, 700 and 900 A, respectively, with a fixed Ar flow rate of 35 l min^{-1} and chamber pressure of 15 kPa. With a given plasma current, the energy input rate shows an approximate parabolic increase with increasing H_2 flow rate. Considering the relative proportions of Ar to H_2 in the plasma gas, H_2 has a much greater contribution to the total plasma energy than Ar, because of its contribution to both dissociation and ionization energy [30]. The energy input rate was found not to be measurably influenced by varying chamber pressure at any given plasma current, Ar and H_2 flow rates.

The experimental measurements in figures 2 to 4 show that the energy input rate increases approximately linearly with increasing plasma current and Ar flow rate, and approximately parabolically with increasing H_2 flow rate. Empirically, therefore, it is proposed that the energy input rate can be expressed as

$$\dot{E} = I(K_1 F_{\mathrm{Ar}} + K_2\sqrt{F_{\mathrm{H_2}}} + K_3) \tag{2}$$

where I is plasma current, F_{Ar} is Ar flow rate, $F_{\mathrm{H_2}}$ is H_2 flow rate, and K_1, K_2 and K_3 are

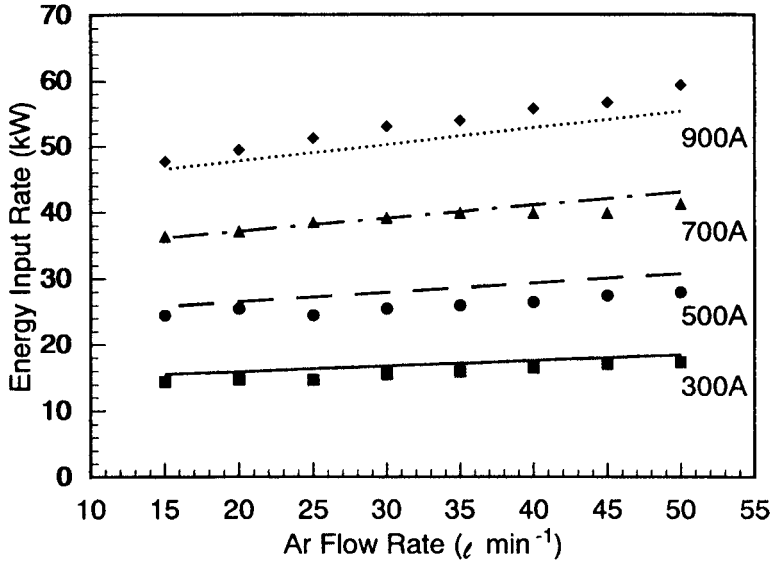

Figure 3. Relationship between plasma energy input rate and Ar flow rate.

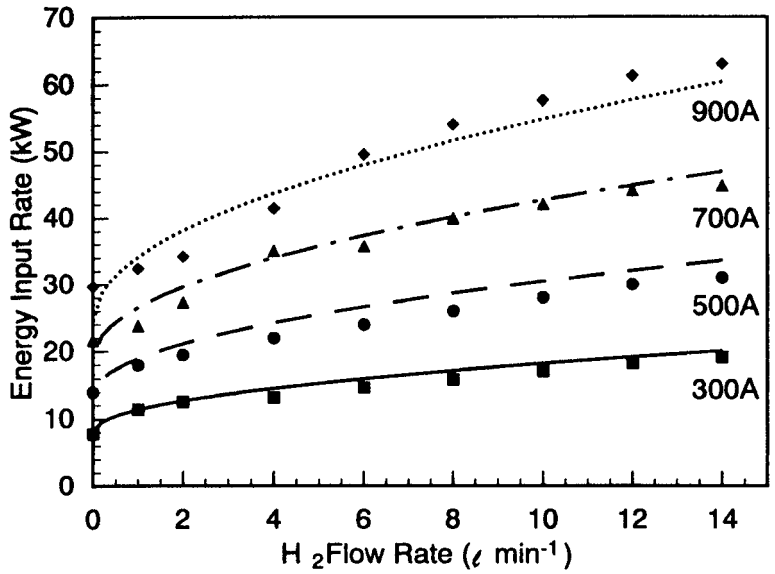

Figure 4. Relationship between plasma energy input rate and H_2 flow rate.

constants. Best-fitting equation (2) to all the experimental measurements in figures 2 to 4 gives the constants $K_1 = 413.3$ V s mol^{-1}, $K_2 = 407.6$ V s$^{-1/2}$ mol$^{-1/2}$ and $K_3 = 17.39$ V, after conversion of flow rates from l min^{-1} to mol s^{-1}. The best fit values of the energy input rate calculated from equation (2) as functions of plasma current, Ar flow rate and H_2 flow rate are superimposed on the experimental data in figures 2, 3 and 4. Figure 5 shows the overall relationship between the best fit values calculated from equation (2) for all the experimental measurements of the energy input rate, with an overall error $<10\%$.

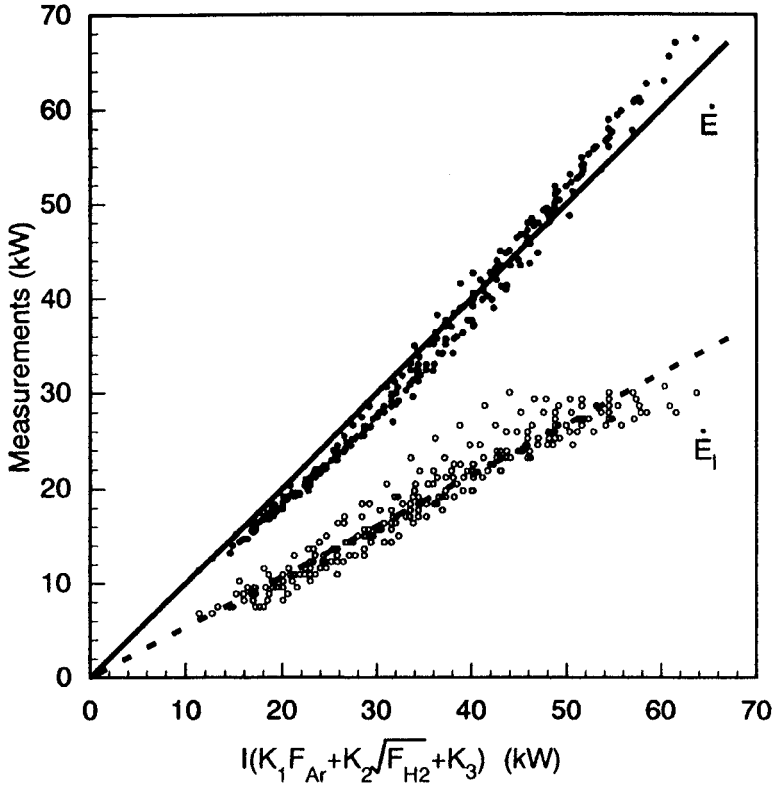

Figure 5. Relationship between measurements for energy input rate and energy loss rate and calculations using equation (2).

3.3. Energy loss rate $\dot{E}_l$

Neglecting radiation, the energy loss rate $\dot{E}_l$ is the thermal loss through the plasma gun to the plasma gun cooling water and can be calculated by

$$\dot{E}_l = C_w F_w (T_w - T_{w_0}) \tag{3}$$

where $C_w = 75.24$ J mol^{-1} K^{-1} [31] is the specific heat of water, F_w is the molar flow rate of the plasma gun cooling water, and T_w and T_{w_0} are the temperatures of the cooling water leaving and entering the plasma gun, respectively. For a series of VPS processing conditions, F_w, T_w and T_{w_0} were measured experimentally, and the energy loss rates in each case were determined from equation (3). Figure 5 shows that the energy loss rate from the plasma gun is typically 50–60% of the total energy input rate under a given processing condition, with an overall average of ∼54%. Therefore, the energy loss rate as a function of processing parameters may be approximated by

$$\dot{E}_l = 0.54\dot{E} = 0.54I(K_1 F_{Ar} + K_2\sqrt{F_{H_2}} + K_3). \tag{4}$$

3.4. Dissociation and ionization energy consumption rate $\dot{E}_i$

The dissociation and ionization energy consumption rate $\dot{E}_i$ of a gas mixture of Ar and H_2 heated to temperature T can be calculated by

$$\dot{E}_i = \chi_{Ar} Q_{Ar} + \chi_{H_2} F_{H_2} Q_{H_2} + 2\chi_H \chi_{H_2} F_{H_2} Q_H \tag{5}$$

where χ_{Ar} and χ_{H} are the Ar and H degrees of ionization, χ_{H_2} is the H_2 degree of dissociation, $Q_{Ar} = 1.5206 \times 10^6$ J mol^{-1} and $Q_{H} = 1.3117 \times 10^6$ J mol^{-1} are the Ar and H ionization energies, respectively, and $Q_{H_2} = 4.320 \times 10^5$ J mol^{-1} is the H_2 dissociation energy [32]. The degree of dissociation or ionization is the ratio of the number of dissociated molecules or ionized atoms to the number of the initial molecules or atoms, respectively.

The ionization of gases can be regarded as quasi-chemical reversible reactions. Saha analysed the thermodynamic equilibrium constant of such a reaction and developed a well known equation to describe the degree of ionization as a function of temperature, pressure and ionization energy [28]. The degree of dissociation of a diatomic gas into two monatomic atoms can also be described by the Saha equation with a different coefficient specific to the dissociation reaction [28, 29]. The degree of dissociation or ionization χ can therefore be assumed to follow the Saha equation [28, 29]

$$\frac{\chi^2}{1-\chi^2} = \frac{kT^{2.5}}{P} e^{-Q/RT} \tag{6}$$

where, $k = k_i = 0.032$ Pa K$^{-2.5}$ for all ionization, $k = k_d = 17.97$ Pa K$^{-2.5}$ for H_2 dissociation, P is the plasma gas pressure, T is the plasma gas temperature assuming local thermodynamic equilibrium, Q is the dissociation or ionization energy and $R = 8.31$ J K^{-1} mol^{-1} is the gas constant.

Substituting equation (6) into equation (5) gives the dissociation and ionization energy consumption rate as

$$\dot{E}_i = F_{Ar} Q_{Ar} \left(1 + \frac{P e^{Q_{Ar}/RT}}{k_i T^{2.5}}\right)^{-1/2} + F_{H_2} \left(1 + \frac{P e^{Q_{H_2}/RT}}{k_d T^{2.5}}\right)^{-1/2} \left[Q_{H_2} + 2Q_H \left(1 + \frac{P e^{Q_H/RT}}{k_i T^{2.5}}\right)^{-1/2}\right]. \tag{7}$$

3.5. Heating energy consumption rate $\dot{E}_h$

The energy consumption rate $\dot{E}_h$ to heat a gas mixture of Ar and H_2 from room temperature $T_r = 298$ K to a temperature T is given by

$$\dot{E}_h = \int_{T_r}^{T} (F_{Ar} C_{Ar} + F_{H_2} C_{H_2}) \, dT \tag{8}$$

where C_{Ar} and C_{H_2} (J mol^{-1} K^{-1}) are the specific heats of Ar and H_2, respectively, and are given as functions of the temperature by [33, 34]

$$C_{Ar} = 20.79 - 3.2 \times 10^{-5} T + 5.16 \times 10^{-8} T^2 \tag{9}$$

$$C_{H_2} = 20.28 - 3.260 \times 10^{-3} T + 5.0 \times 10^{4} T^{-2}. \tag{10}$$

Substituting equations (9) and (10) into equation (8) and integrating gives the heating energy consumption rate as

$$\dot{E}_h = (6194.45 + 20.79T - 1.6 \times 10^{-5} T^2 + 1.72 \times 10^{-8} T^3) F_{Ar} + (6391.22 + 27.28T - 1.630 \times 10^{-3} T^2 - 5.0 \times 10^{4} T^{-1}) F_{H_2}. \tag{11}$$

3.6. Initial plasma gas temperature

It can be seen from equations (2), (4), (7) and (11) that $\dot{E}$, $\dot{E}_1$, $\dot{E}_i$ and $\dot{E}_h$ are all functions of VPS processing parameters and plasma temperature. For a given set of plasma current,

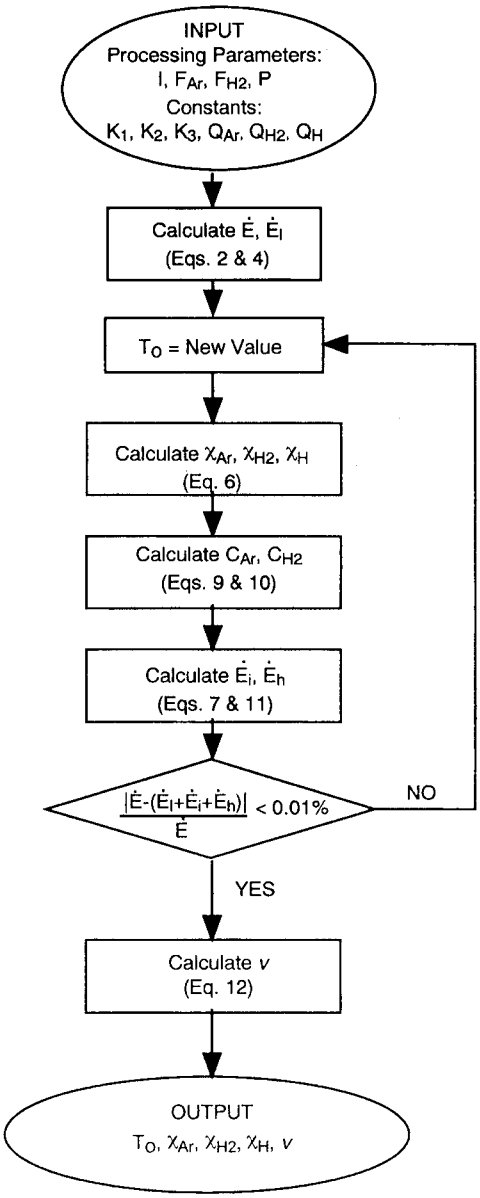

Figure 6. Flow diagram of numerical procedure for calculation of initial plasma properties.

plasma gas flow rates and chamber pressure, the initial plasma temperature T_0 at the plasma gun exit can be determined by substituting equations (2), (4), (7) and (11) into equation (1), in which plasma temperature is the only unknown variable. Equation (1) cannot be solved explicitly, so the initial plasma temperature T_0 and the corresponding degrees of ionization and dissociation were determined iteratively to within 0.01% using a BASIC program with the algorithm shown schematically in figure 6.

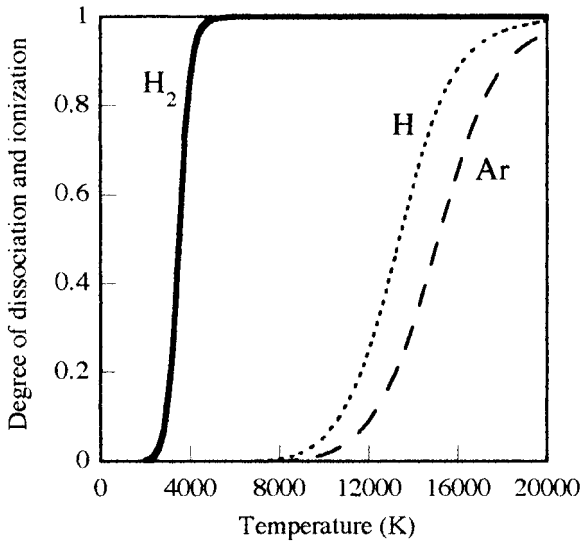

Figure 7. Relationship between degrees of H_2 dissociation, and Ar and H ionization and plasma gas temperature ($P = 15$ kPa).

3.7. Initial plasma gas velocity

Within the plasma gun, the molar flow rates of atomic gases remain constant through all cross sections regardless of variations in gas temperature and velocity, while the molar flow rates of diatomic gases at the gun exit orifice double from their internal value if dissociation is complete. Figure 7 shows the degrees of H_2 dissociation, and Ar and H ionization as functions of the gas temperature at a gas pressure of 15 kPa, as calculated from equation (6). When the plasma gas temperature is above 6000 K, the H_2 dissociation is nearly complete for a gas pressure below the atmospheric pressure. Assuming ideal gas behaviour, the initial gas velocity v at the plasma gun exit orifice for temperatures >6000 K is therefore given by

$$v = \frac{RT_0(F_{\mathrm{Ar}} + 2F_{\mathrm{H_2}})}{P_0 S} \tag{12}$$

where P_0 is the plasma gas pressure at the plasma gun exit orifice and S is the cross sectional area of the plasma gun exit orifice. P_0 is assumed to be equal to the chamber pressure [35].

4. Predicted effects with varying VPS conditions

4.1. Plasma current

Figures 8(a)–(c) show variations of initial plasma gas temperature, degrees of Ar and H ionization and plasma gas velocity, respectively, with plasma current in the range 400–1000 A, at a fixed Ar flow rate of 35 l min^{-1}, H_2 flow rate of 8 l min^{-1} and chamber pressure of 15 kPa. As the calculated plasma gas temperatures in these conditions are above 9000 K, H_2 dissociation is virtually complete and equation (12) is applicable. With increasing plasma current from 400 to 1000 A, the plasma energy input rate increases linearly as shown by equation (2) and the calculated plasma temperature, degrees of Ar and H ionization and plasma gas velocity show strong increases in the range 9200 to 13 300 K, 0.01 to 0.2, 0.03 to 0.48, and 1560 to 2260 m s^{-1}, respectively, as shown in figures 8(a), (b) and (c).

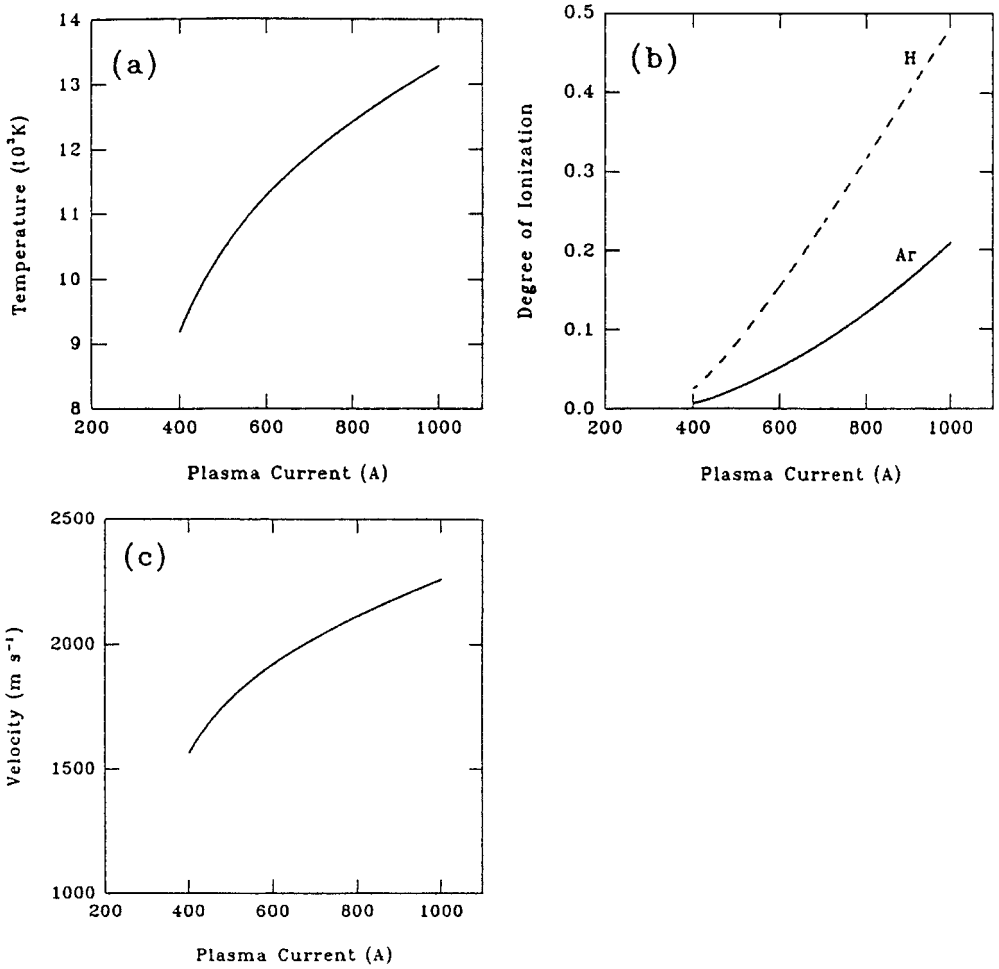

Figure 8. Effect of plasma current on: (a) plasma gas temperature, (b) degree of Ar and H ionization and (c) plasma gas velocity.

4.2. Ar flow rate

Figures 9(a)–(c) show variations of initial plasma gas temperature, degrees of Ar and H ionization and plasma gas velocity, respectively, with Ar flow rate in the range 15–50 l min^{-1}, at a fixed plasma current of 700 A, H_2 flow rate of 8 l min^{-1} and chamber pressure of 15 kPa. With increasing Ar flow rate from 10 to 100 l min^{-1} the plasma energy input rate increases linearly as shown by equation (2). However, the initial plasma gas temperature and degrees of Ar and H ionization all decrease significantly from 13 100 to 10 300 K, 0.2 to 0.02 and 0.45 to 0.08, respectively, as shown in figures 9(a) and (b), because the quantity of plasma gas to be heated increases at a faster rate than the plasma energy input. In contrast, the gas velocity increases almost linearly from ∼1200 to 4000 m s^{-1} over the range, as shown in figure 9(c).

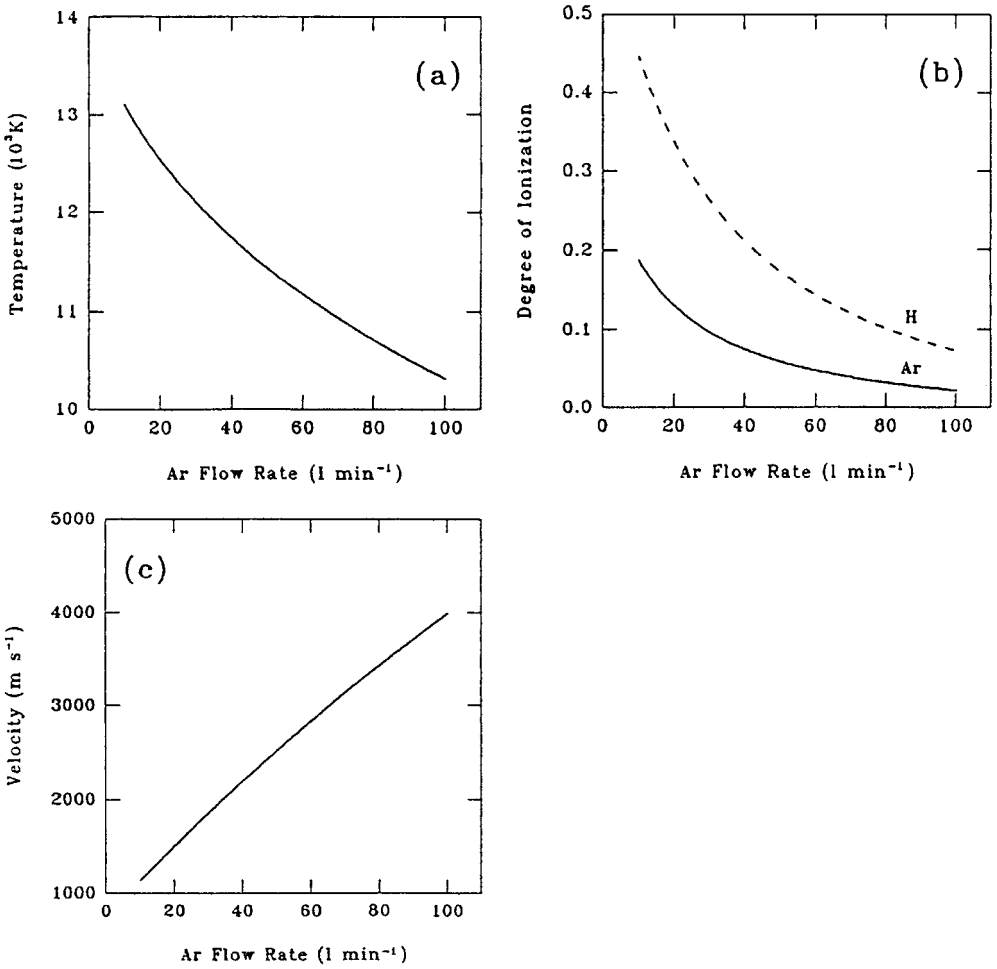

Figure 9. Effect of Ar flow rate on: (a) plasma gas temperature, (b) degree of Ar and H ionization and (c) plasma gas velocity.

4.3. H_2 *flow rate*

Figures 10(a)–(c) show variations of the initial plasma gas temperature, degrees of Ar and H ionization and plasma gas velocity, respectively, with H_2 flow rate in the range 0–20 l min^{-1}, at a fixed plasma current of 700 A, Ar flow rate of 35 l min^{-1} and chamber pressure of 15 kPa. H_2 is often used in VPS as a secondary gas because its dissociation and ionization contribute strongly to the overall plasma enthalpy [1, 25]. With fixed plasma current, Ar flow rate and chamber pressure, increasing the H_2 flow rate increases the plasma energy input rate parabolically, as shown by equation (2). Initially, small additions of secondary H_2 up to 2 l min^{-1} increases both the initial plasma gas temperature and the degrees of Ar and H ionization, as shown in figures 10(a) and (b), respectively. However, as the H_2 flow rate increases above 2 l min^{-1}, the volume of gas to be heated per unit time increases at a faster rate than the plasma energy input rate. The initial plasma gas temperature and degrees of Ar and H ionization then decrease with increasing H_2 flow rate, as shown in figures 10(a) and (b), respectively. Figure 10(c) shows

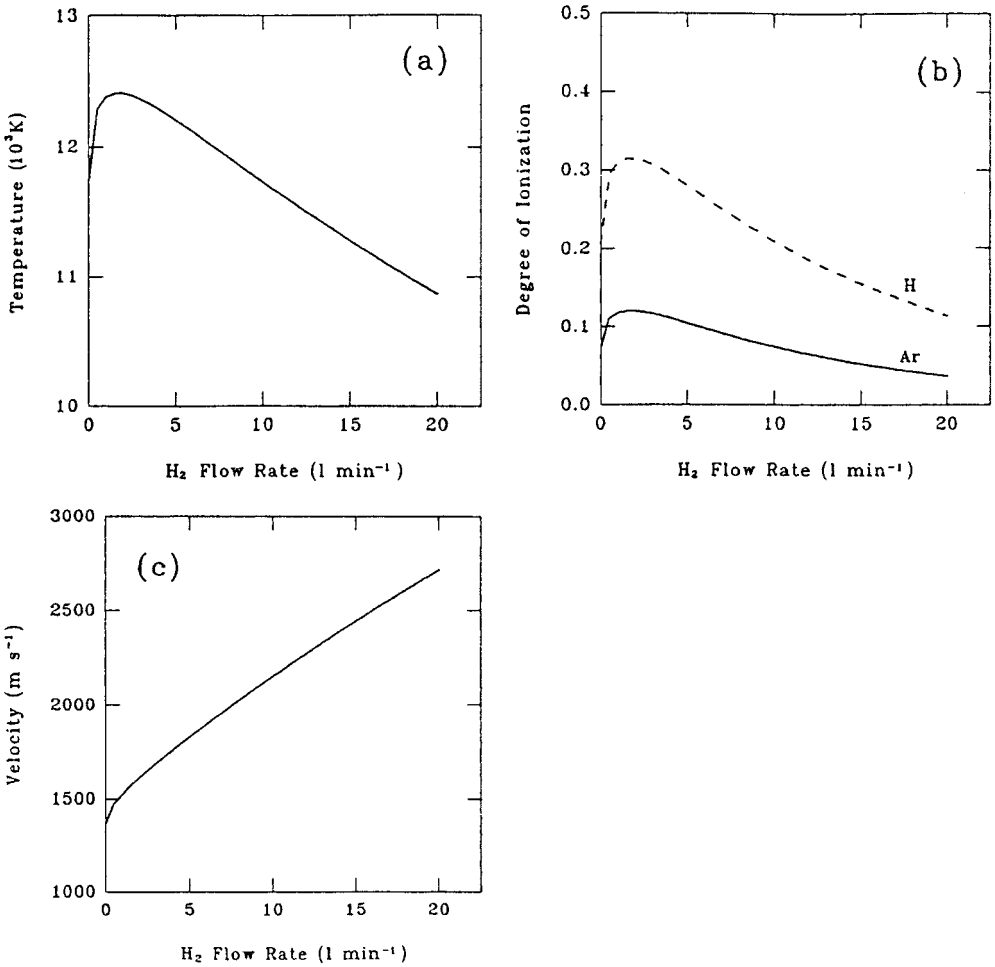

Figure 10. Effect of H_2 flow rate on: (a) plasma gas temperature, (b) degree of Ar and H ionization and (c) plasma gas velocity.

that the plasma gas velocity increases almost linearly with increasing H_2 flow rate, from about 1400 m s^{-1} without secondary H_2 to 2750 m s^{-1} at a H_2 flow rate of 20 l min^{-1}.

4.4. Chamber pressure

Figures 11(a)–(c) show variations of initial plasma gas temperature, degrees of Ar and H ionization and plasma gas velocity, respectively, with chamber pressure in the range 2.5–100 kPa, at a fixed plasma current of 700 A, Ar flow rate of 35 l min^{-1} and H_2 flow rate of 8 l min^{-1}. The plasma gas pressure at the plasma gun exit is usually equal to the chamber pressure [35]. According to equation (2), chamber pressure alone has no effect on the plasma energy input rate. The energy consumed by dissociation and ionization of the plasma gases, however, decreases with increasing chamber pressure as shown in equation (7), because the degrees of Ar and H ionization decrease, as shown in figure 11(b). Figure 11(a) shows that the plasma gas temperature increases moderately with increasing chamber pressure because the energy consumption in dissociation and ionization decreases and consequently

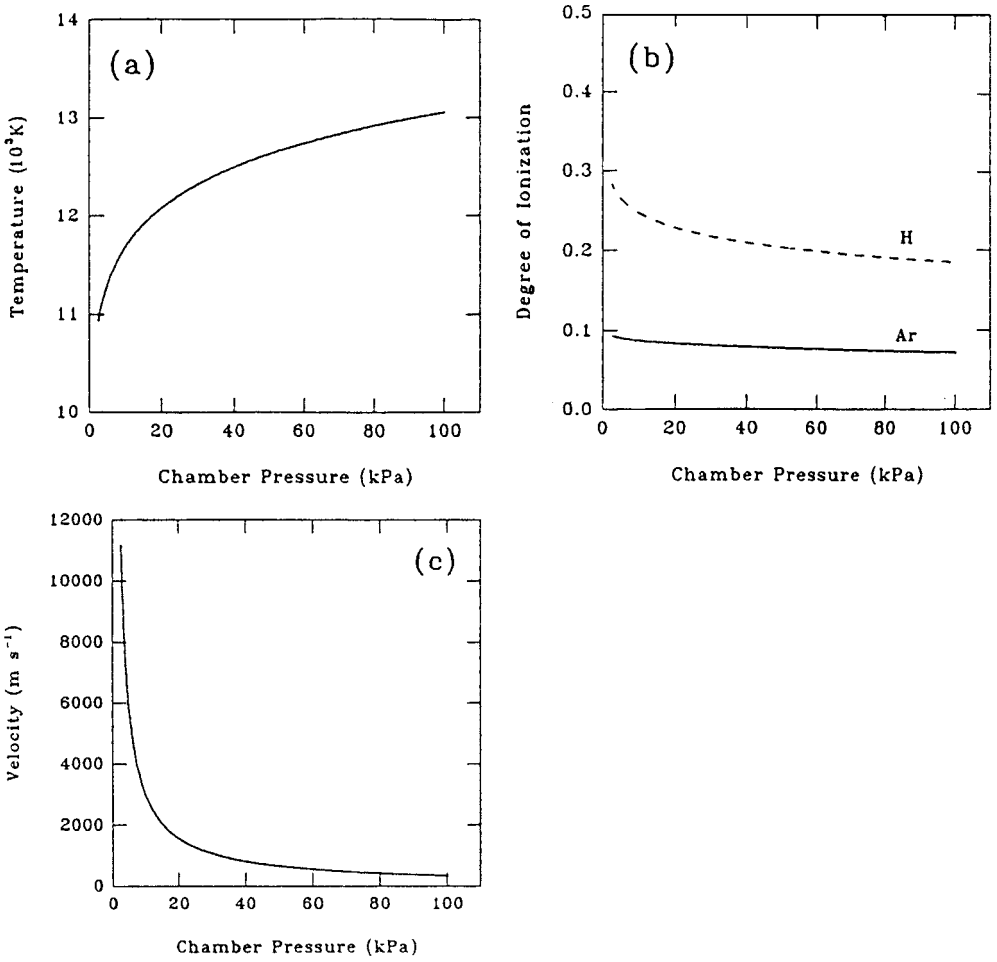

Figure 11. Effect of chamber pressure on: (a) plasma gas temperature, (b) degree of Ar and H ionization and (c) plasma gas velocity.

the energy available for heating increases. Figure 11(c) shows that the plasma gas velocity decreases rapidly with increasing chamber pressure as expected from equation (12). The chamber pressure has a particularly strong effect on the gas velocity below ~20 kPa, but little subsequent effect above ~20 kPa.

5. Discussion

The initial plasma gas temperature, degrees of dissociation and ionization, and plasma gas velocity predicted from equations (1), (6) and (12), respectively, are in reasonable agreement with previous calculations and measurements in the literature [9, 15, 16, 19, 36]. For example, Fauchais *et al* [19] reported a temperature at the plasma gun exit of 14 000 K and velocity of ~900 m s^{-1} for a 29 kW Ar–H_2 plasma jet, and similar to the present predictions of 10 000–13 000 K and 500–2500 m s^{-1}. It should be noted that the model cannot be applied directly to plasma guns other than PT-A2000. The constants K_1, K_2 and K_3 in equation (2), the

ratio between the energy loss rate $\dot{E}_l$ and the energy input rate $\dot{E}$, and the cross sectional area of the plasma gun orifice S in equation (12) are all gun dependent and need to be determined experimentally for each plasma gun.

However, there are assumptions in the model calculations which are potential sources of error.

(1) The plasma gas is assumed to be in local thermodynamic equilibrium, although deviations are sometimes observed. For example, when the chamber pressure is lower than 1×10^4 Pa, the electron temperature is higher than the ion and gas temperatures [26]. Nonetheless, for the range of VPS operating conditions in this study, the plasma gas may be reasonably assumed to be close to local thermodynamic equilibrium [26].
(2) The degrees of plasma gas dissociation and ionization as functions of temperature and pressure are assumed to follow the Saha equation (6), which is applicable for a given gas at thermodynamic equilibrium [28, 29], but not necessarily for two or more gases at non-uniformly distributed temperatures.
(3) The plasma gas specific heat capacity is assumed to be a mixture of those of Ar and H_2 in proportion to their flow rates, which may not always be accurate for highly ionized gases at temperatures up to 16 000 K.
(4) All energy losses in the plasma gun are assumed to be removed by the cooling water. In practice, energy losses include not only those by heat transfer to the plasma gun nozzle itself and the cooling water but also radiation losses. The energy radiated per unit time per unit volume by a fully ionized plasma is proportional to the square root of the plasma temperature and is usually less than 15% of the plasma energy input rate when plasma temperature is below 15 000 K [37]. A considerable amount of the radiated heat may also be reabsorbed by the plasma gas downstream from the nozzle.
(5) The plasma is assumed to obey the ideal gas law, but non-ideal behaviour is possible in a highly ionized plasma.
(6) Plasma gas temperature and velocity are assumed to be constant across the nozzle exit. In practice, there are steep temperature and velocity gradients because of boundary layer effects near the nozzle wall [16, 20].

Overall, therefore, the present calculations of initial plasma gas temperature, degrees of dissociation and ionization and plasma gas velocity should not be expected to be too accurate. Quantitative assessment of the accuracy of the calculations needs direct comparison with experimental measurements. Nonetheless, in the absence of readily available measurement techniques and data the calculations are useful to predict the trends of variations with VPS operating conditions. In this study, the main application of these calculations are described in part II where the predictions of plasma gun exit conditions are used as boundary conditions for a computational fluid dynamics model of subsequent chamber and particle flow during VPS.

6. Conclusions

The measured plasma energy input rate of a dc Ar + H_2 plasma jet increases approximately linearly with increasing plasma current I and Ar flow rate F_{Ar}, and approximately parabolically with increasing H_2 flow rate F_{H_2}. Empirically, the energy input rate can be expressed as

$$\dot{E} = I(K_1 F_{Ar} + K_2 \sqrt{F_{H_2}} + K_3)$$

where K_1, K_2 and K_3 are constants dependent on plasma gun geometry and plasma gas properties.

An analytical model has been developed to calculate the initial plasma gas temperature, degrees of Ar and H ionization and plasma gas velocity at the plasma gun exit as functions of the VPS processing parameters of plasma current, Ar flow rate, H_2 flow rate and chamber pressure, based on an energy balance between the electrical input energy and the energy consumed by thermal losses, plasma gas dissociation and ionization, and plasma gas heating. The model predicts:

(1) increasing the plasma current increases the initial plasma gas temperature, the degrees of Ar and H ionization, and the plasma gas velocity;
(2) increasing the Ar flow rate decreases the initial plasma gas temperature and the degrees of Ar and H ionization, but increases the initial plasma gas velocity;
(3) increasing the H_2 flow rate increases and then decreases the initial plasma gas temperature and the degrees of Ar and H ionization, with peak values at about 2 l min^{-1}, and increases the initial plasma gas velocity; and
(4) increasing the chamber pressure increases the initial plasma gas temperature, decreases the degrees of Ar and H ionization slightly, and strongly decreases the plasma gas velocity.

Acknowledgments

We would like to thank The UK Engineering and Physical Sciences Research Council, The British Council, The Chinese Education Commission and The Royal Society for financial support.

References

[1] Dearnley P A and Roberts K A 1991 *Powder Metall.* **34** 23
[2] Zhao Y Y, Grant P S and Cantor B 1993 *J. Physique* IV **3** 1685
[3] Grant P S, Zhao Y Y, Li J H, Jenkins M L and Cantor B 1995 *Science and Technology of Rapid Solidification and Processing Technologies* ed M A Otooni (Netherlands: Kluwer) p 109
[4] Zhao Y Y, Grant P S and Cantor B 1995 *Recent Advances in Titanium Metal Matrix Composites* ed F H Froes and J Storer (Pennsylvania: TMS) p 55
[5] Grant P S, Hambleton R, Zhao Y Y, O'Reilly K A Q and Cantor B 1995 *Surface Modification Technologies VIII* ed T S Sudarshan and M Jeadin (London: The Institute of Materials) p 783
[6] Fan Z, Grant P S and Cantor B 1997 *Key Eng. Mater.* **127–131** 335
[7] Baik K-H and Grant P S 1997 *Proc. 5th Eur. Conf. on Advanced Materials, Processes and Applications* vol 1, ed L A J Sarton and H B Zeedijk (Zwijndrecht, Netherlands: Bond voor Materialenkennis) p 341
[8] Baik K-H and Grant P S 1998 *Thermal Spray, Meeting the Challenges of the 21st Century* ed C Coddet (Novelty, OH: ASM) p 1193
[9] Apelian D *et al* 1983 *Int. Metals Rev.* **28** 271
[10] Grant P S *et al* 1989 *Scripta Metall.* **23** 1651
[11] Steffens H D and Dvorak M 1991 *Thermal Spray Research and Applications* ed T Bernecki (Novelty, OH: ASM) p 207
[12] Smith R W 1991 *Proc. 2nd Plasma-Technik-Symposium* vol 1 (Wohlen, Switzerland: Plasma-Technik AG) p 17
[13] MacKay R A, Brindley P K and Froes F H 1991 *JOM* **43** 23
[14] Wei D, Apelian D and Farouk B 1985 *Proc. 7th Int. Symp. on Plasma Chem.* ed C J Timmermans (New York: Pergamon) p 810
[15] Takeda K, Hayashi K and Ohashi T 1985 *Proc. 7th Int. Symp. on Plasma Chem.* ed C J Timmermans (New York: Pergamon) p 848
[16] Dilawari A H and Szekely J 1987 *Plasma Processing and Synthesis of Materials* ed D Apelian and J Szekely (Pittsburgh, PA: Materials Research Society) p 3
[17] McKelliget J W and El-Kaddah N 1987 *Plasma Processing and Synthesis of Materials* ed D Apelian and J Szekely (Pittsburgh, PA: Materials Research Society) p 21
[18] Vardelle M *et al* 1987 *Proc. 8th Int. Symp. on Plasma Chem.* vol 1, ed K Akashi and A Kinbara (Research Triangle Park, NC: International Union of Pure & Appl. Chem.) p 404

[19] Fauchais P *et al* 1989 *Metall. Trans.* B **20** 263
[20] Pfender E, Chen W L T and Spores R 1991 *Thermal Spray Research and Applications* ed T Bernecki (Novelty, OH: ASM) p 1
[21] Hedges M A and Taylor R 1991 *Thermal Spray Research and Applications* ed T Bernecki (Novelty, OH: ASM) p 59
[22] Fincke J R *et al* 1994 *Int. J. Heat Mass Transfer* **37** 1673
[23] Fauchais P *et al* 1988 *Thermal Spray: Advances in Coatings Technology* ed D L Houck (Metals Park, OH: ASM) p 11
[24] Pfender E 1988 *Surf. Coatings Technol.* **1** 1
[25] Herman H 1988 *Mater. Res. Soc. Bull.* **13** 60
[26] Hoyaux M F 1968 *Arc Physics* (New York: Springer) p 35
[27] Goldman A and Amouroux J 1983 *Electrical Breakdown and Discharges in Gases Part B: Macroscopic Processes and Discharges* ed E E Kunhardt and L H Luessen (New York: Plenum) p 293
[28] Howatson A M 1965 *An Introduction to Gas Discharges* (Oxford: Pergamon) pp 114–17
[29] Kubin R F and Presley L L 1964 *Thermodynamic Properties and Mollier Chart for Hydrogen from 300 K to 20 000 K* (Washington DC: NASA) pp 4, 5 and 20
[30] Gill S C and Clyne T W 1991 *Proc. 2nd Plasma-Technik-Symposium* (Wohlen, Switzerland: Plasma-Technik AG) p 227
[31] Lide D R 1996 *CRC Handbook of Chemistry and Physics* 77th edn (Boca Raton, FL: CRC Press) section 6, pp 6–8
[32] Matejka D and Benko B 1989 *Plasma Spraying of Metallic and Ceramic Materials* (New York: Wiley) p 26
[33] Reid R C, Prausnitz J M and Sherwood T K 1977 *The Properties of Gases and Liquids* 3rd edn (New York: McGraw-Hill) p 629
[34] Atkins P W 1982 *Physical Chemistry* 2nd edn (Oxford: Oxford University Press) p 111
[35] Cheers F 1963 *Elements of Compressible Flow* (London: Wiley) p 95
[36] Wei D Y C, Apelian D and Farouk B 1987 *Plasma Processing and Synthesis of Materials* ed D Apelian and J Szekely (Pittsburgh, PA: Materials Research Society) p 77
[37] Arzimovich L A 1965 *Elementary Plasma Physics* (New York: Blaisdell) p 81